Draft version August 7, 2022
Typeset using LaTeX **twocolumn** style in AASTeX631

Chemistry of the most metal-poor DLA currently known

Louise Welsh [1,2] Ryan Cooke [3] Michele Fumagalli [1,4] and Max Pettini [5]

[1] *Dipartimento di Fisica G. Occhialini, Università degli Studi di Milano Bicocca, Piazza della Scienza 3, I-20126 Milano, Italy*
[2] *INAF – Osservatorio Astronomico di Brera, via Bianchi 46, I-23087 Merate (LC), Italy*
[3] *Centre for Extragalactic Astronomy, Durham University, South Road, Durham DH1 3LE, UK*
[4] *INAF - Osservatorio Astronomico di Trieste, via G. B. Tiepolo 11, I-34143 Trieste, Italy*
[5] *Institute of Astronomy, University of Cambridge, Madingley Road, Cambridge CB3 0HA, UK*

ABSTRACT

Keywords: Damped Lyman-alpha systems (349); Intergalactic medium (813); Population III stars (1285); Population II stars (1284); Chemical abundances (224)

1. INTRODUCTION

Tracing chemical evolution from the Cosmic Dawn at $z \sim 15-30$ to the present epoch is a key goal of modern astronomy. Reservoirs of gas, detected in absorption along the line of sight towards unrelated background quasars, are of particular use in this endeavour. These low density structures allow us to trace the evolution of metals from $0 < z < 5$ with a consistent degree of sensitivity (Péroux & Howk 2020). The largest of these absorption line systems, whose column density of neutral hydrogen exceeds $\log_{10} N(\mathrm{H\,I})/\mathrm{cm}^{-2} > 20.3$ are known as Damped Lyα systems (DLAs; see Wolfe et al. 2005 for a review). These DLAs are uniquely suited to high-precision chemical abundance studies; the large column density of neutral hydrogen means that the gas is optically thick to ionising radiation and the constituent metals reside in a single, dominant ionisation state. This negates the need for ionisation corrections and the column density of the observed ionic species can be used to precisely determine the relative metal abundances of the gas reservoir.

Often we describe these systems by their metallicity. In principle, this property is easily defined as the the amount of metals in system relative the hydrogen content. This is often expressed as [X/H] where this denotes the logarithmic number abundance ratio of elements X and H relative to their solar values $\mathrm{X}_\odot$ and $\mathrm{Y}_\odot$, i.e. $[\mathrm{X/Y}] = \log_{10}(N_\mathrm{X}/N_\mathrm{Y}) - \log_{10}(N_\mathrm{X}/N_\mathrm{Y})_\odot$. However, the metal (or combination of metals) used in this expression is dependent on the system being analysed and, ultimately, on the accessible features. It is typical to use a combination of Fe and α elements. As we go towards the low metallicity tail of objects, peculiar chemical abundance patterns become more apparent. This is well documented in the analysis of metal-poor Milky Way halo stars where the paucity of Fe is often associated with an overabundance of C. These objects are known as carbon enhanced metal-poor stars (CEMP; see Beers & Christlieb 2005). When C is detected in excess alongside a minimal contribution from Fe, [Fe/H] fails to describe the overall metal-paucity of the object/system in question.

There is the potential detection of an UMP DLA at $z \sim 7$ (Simcoe et al. 2012). Though, at this redshift it extremely challenging to detect the distinctive damped absorption from neutral hydrogen that is characteristic of DLAs[1].

The DLA found towards the quasar SDSS J090333.55+262836.3 (hereafter J0903+2628) is the *most* metal-poor DLA currently known (Cooke et al. 2017). This was determined through the analysis of absorption from low ionic species such as C II, O I, Si II, and Fe II. The previously accessible Fe II features were restricted to the weak Fe II λ1260 transition. The was necessary to observe the absorption due to the lighter atomic number elements alongside the associated H I.

Corresponding author: Louise Welsh
louise.welsh@unimib.it

[1] We refer the reader to Bosman & Becker (2015) for an alternative interpretation of these data and the sensitivity of the detection on modelling the QSO emission.

Given the extreme metal-paucity of this system, we have sought additional high resolution observations that target the stronger Fe II λ1608 and Fe II λ2382 features. These observations also target the Al II λ1670 features — providing the first insight into the abundance of odd-atomic number elements for this DLA. The results of these observations and the subsequent data analysis are the subject of this paper.

This paper is organised as follows. Section 2 describes our observations and data reduction. In Section 3, we present our data and an updated chemical composition this DLA. We discuss the chemical enrichment history of this system in Section 4, before drawing overall conclusions and suggesting future work in Section 5.

2. OBSERVATIONS AND DATA REDUCTION

J0903+2628 has previously been identified as the most metal-poor DLA currently known. We have a acquired an additional 10 hours of echelle spectroscopy on the associated quasar using Keck I/HIRESr. We do no use the last exposure due to cloud conditions. The flux profile suggests that the QSO may not have been centred on the slit for this final OB (possibly an issue towards the end of the penulitmate OBs too).

The HIRES data were reduced with the HiresREDUX reduction pipeline. This pipeline include the standard reduction steps of subtracting the detector bias, locating and tracing the echelle orders, flat-fielding, sky subtraction, optimally extracting the 1D spectrum, and performing a wavelength calibration. The data were converted to a vacuum and heliocentric reference frame.

Finally, we combined the individual exposures of this DLA using UVES_POPLER[2]. This corrects for the blaze profile, and allowed us to manually mask cosmic rays and minor defects from the combined spectrum. When combining these data we adopt a pixel sampling of 2.5 km s^{-1}.

3. ANALYSIS

Using the Absorption LIne Software (ALIS) package[3]— which uses a χ-squared minimisation procedure to find the model parameters that best describe the input data — we simultaneously analyse the full complement of high S/N and high spectral resolution data currently available for the DLA towards J0903+2628 . We model the absorption lines with a Voigt profile, which consists of three free parameters: a column density, a redshift, and a line broadening. We assume that all lines of comparable ionization level have the same redshift, and any absorption lines that are produced by the same ion all have the same column density and total broadening. The total broadening of the lines includes a contribution from both turbulent and thermal broadening. The turbulent broadening is assumed to be the same for all absorption features, while the thermal broadening depends inversely on the square root of the ion mass; thus, heavy elements (e.g. Fe) will exhibit absorption profiles that are intrinsically narrower than the profiles of lighter elements, (e.g. C). There is an additional contribution to the line broadening due to the instrument. For these HIRES data, the nominal instrument resolution is $v_{\rm FWHM}$ = 6.28 km s^{-1} (C1). Finally, we note that we simultaneously fit the absorption and quasar continuum of the data. We model the continuum around every absorption line as a low-order Legendre polynomial (typically of order 3). We assume that the zero-levels of the sky-subtracted HIRES data do not depart from zero[4].

The DLA towards J0903+2628 is best modelled by three absorption components for C II and Si II at redshifts: $z_{\rm abs}$ = 3.077589 ± 0.000002, $z_{\rm abs}$ = 3.076653 ± 0.000005, and $z_{\rm abs}$ = 3.076331 ± 0.000006 with. The other detected elements are best modelled by the two highest redshift components only. Due to the blending between the components we cannot directly determine the temperature of the gas reservoir. We therefore assume T = 1.00 × 10^4 K (typical for metal-poor DLAs; see Cooke et al. 2015; Welsh et al. 2020; Noterdaeme et al. 2021). The turbulent broadening of components these components are found to be b = 8.8 ± 0.3 km s^{-1}, b = 9.6 ± 0.5 km s^{-1}, and b = 14.9 ± 0.7 km s^{-1} respectively. The data, along with the best fitting model, are shown in Figure 1 while the resulting column densities and relative abundances are presented in Table 1. We note that the reported abundances allow the relative abundances of metal to vary from component to component. We have repeated our analysis under the assumption that the relative abundances of metals (i.e. the [O/Fe] ratio) must be constant across the components; the resulting total abundances are consistent with those reported in Table 1.

The reported relative abundances are consistent with the previous determination by Cooke et al. (2017).

[2] UVES_POPLER is available from: https://github.com/MTMurphy77/UVES_popler

[3] ALIS is available from: https://github.com/rcooke-ast/ALIS.

[4] We visually inspected the troughs of saturated absorption features to confirm this is the case.

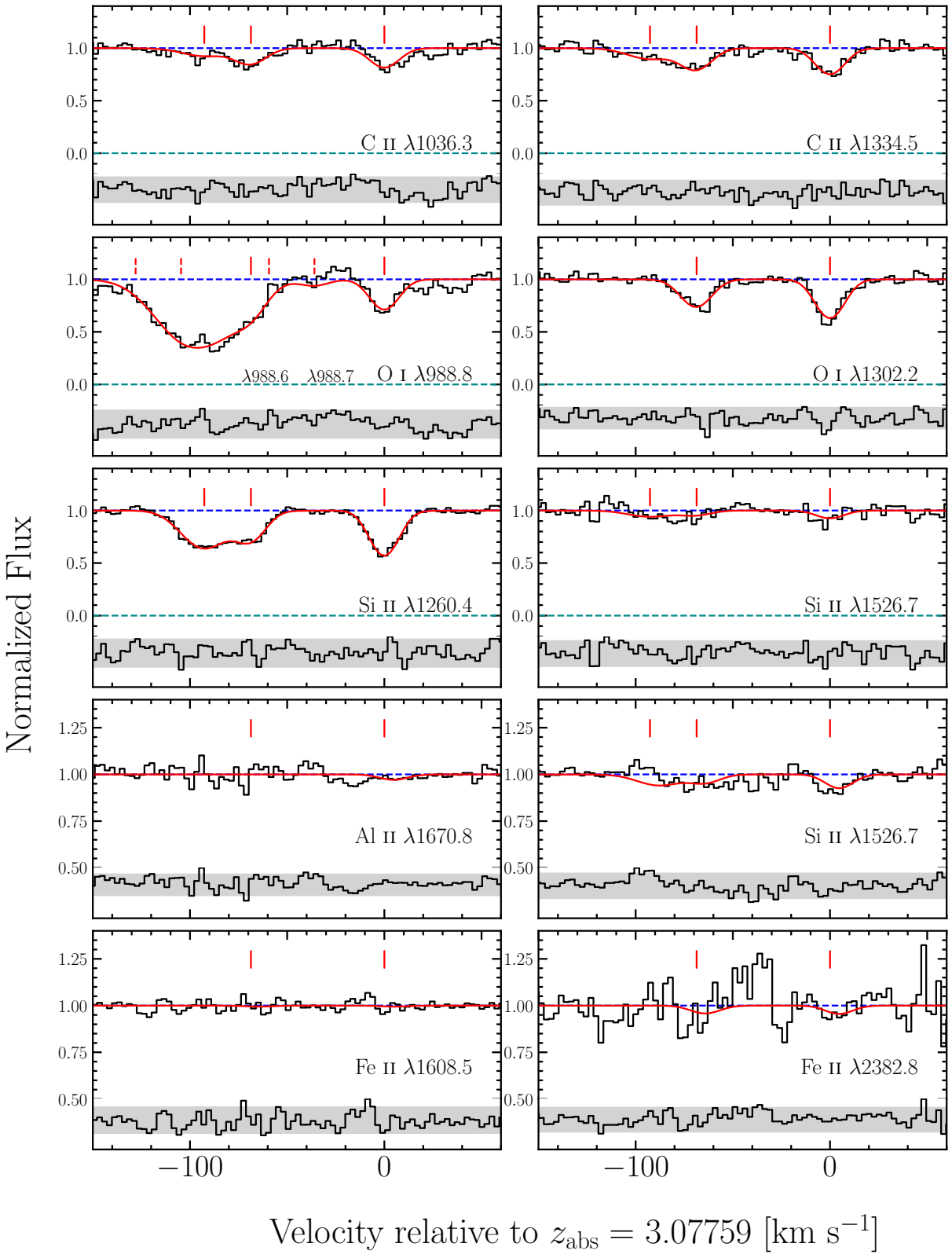

Figure 1. Continuum normalised HIRES data (black histograms) of the absorption features produced by metal ions associated with the DLA at $z_{\rm abs} = 3.077590$ towards the quasar J0903+2628 . The best-fitting model is shown with the red curves. The blue dashed line indicates the position of the continuum while the green dashed line indicates the zero-level. Note the difference scale of the y-axes of the bottom two rows. The red ticks above the absorption features indicate the centre of the Voigt line profiles for each identified component. The dashed-red lines in the third panel highlight the additional features of the O I λ988 triplet. Below the zero-level, we show the residuals of this fit (black histogram) where the grey shaded band encompasses the 2σ deviates between the model and the data.

Table 1. Ion column densities of the DLA at $z_{\rm abs} = 3.07759$ towards the quasar J0903+2628 . The quoted column density errors are the 1σ confidence limits while the column densities are given by $\log_{10} N({\rm X})/{\rm cm}^{-2}$.

Ion	Transitions used [Å]	Solar	Comp. 1 $z_{\rm abs} = 3.077589$	Comp. 2 $z_{\rm abs} = 3.076653$	Comp. 3 $z_{\rm abs} = 3.076331$	Total	[X/H]	[X/Fe]
H I	1215	12.00	—	—	—	20.32 ± 0.05	—	—
C II	1036, 1334	8.43	13.07 ± 0.03	12.99 ± 0.04	12.83 ± 0.06	13.45 ± 0.08	-3.42 ± 0.07	$> +0.24$
O I	988, 1302	8.69	13.70 ± 0.02	13.55 ± 0.03	—	13.93 ± 0.04	-3.08 ± 0.06	$> +0.58$
Al II	1670	6.45	≤ 9.78[a]	≤ 10.97[a]	—	≤ 11.00[a]	≤ -3.76[a]	—
Si II	1260, 1526	7.51	12.40 ± 0.01	12.20 ± 0.03	12.50 ± 0.02	12.86 ± 0.04	-3.22 ± 0.06	$> +0.44$
Fe II	1260, 1608, 2382	7.47	≤ 11.83[a]	≤ 11.83[a]	—	≤ 12.13[a]	≤ -3.66[a]	—

[a] 2σ upper limit on column density.

Total is given by sum of all available components, while abundance ratios consider only the first two components.

Notably, we have improved the upper limit on the [Fe/H] abundance by $\sim$ 1 dex from [Fe/H] < -2.81 to [Fe/H] ≤ -3.66 (2σ). We have also placed the first upper limit on an odd atomic number element, [Al/H] $<\leq -3.76$ (2σ). As will be discussed in subsequent sections, this is a useful indicator of the explosion mechanism of the enriching stellar population. These new data reaffirm that the DLA towards J0903+2628 is the most metal-poor DLA currently known. It has the lowest C, O, Si, and Fe abundance determination of any known DLA.

We look for absorption due to Si III so that we can determine the ionisation ratio and subsequently model the density of the gas reservoir. However, the strong Si III λ1206 features is heavily blended with unrelated absorption.

3.1. *Chemical enrichment model*

Using the [C/O], [Si/O], [Fe/O], and [Al/O] abundance ratios (or the associated upper limits) we use the stochastic chemical enrichment model described in Welsh et al. (2019) to investigate the possible enrichment history of this absorption line system. The basis of this model is described below.

3.1.1. *Likelihood modelling technique*

The mass distribution of metal-free stars is modelled as a power-law: $\xi(M) = k\,M^{-\alpha}$, where α is the power-law slope ($\alpha = 2.35$ for a Salpeter IMF[5]), and k is a multiplicative constant that is set by defining the number of stars, $N_\star$, that form between a minimum mass $M_{\rm min}$ and maximum mass $M_{\rm max}$, given by:

$$N_\star = \int_{M_{\rm min}}^{M_{\rm max}} kM^{-\alpha} dM \ . \tag{1}$$

In this work, $N_\star$ represents the number of stars that have contributed to the enrichment of a system. In addition to the mass distribution, we also consider the typical SN explosion energy of the enriching stars $E_{\rm exp}$, which is a measure of the kinetic energy of the SN ejecta at infinity, and the degree of mixing between the stellar layers during the explosive nuclear burning $f_{\rm He}$, parameterised as a fraction of the He core size.

Using the observed abundances of J0903+2628 we can investigate the likelihood of a given enrichment model by calculating the probability of the observed abundance ratios, R_o, given the abundance ratios expected from that enrichment model, R_m:

$$\mathcal{L} = p(R_o|R_m) \ . \tag{2}$$

The probability of an observed combination of abundance ratios is given by

$$p\big(R_o|R_m\big) = \int p\big(R_o|R_i\big)p\big(R_i|R_m\big)\mathrm{d}R_i \ . \tag{3}$$

The first term of this integral describes the probability of a given observation being equal to the intrinsic abundance ratio of the system, R_i. For abundances with known errors, this distribution is modelled by a Gaussian, where the spread is given by the observational error on the chemical abundance ratio. For abundances with upper limits, this distribution is modelled as a Gaussian convolved with a step function about the 3σ column density limit i.e. :

$$p\big(R_o|R_i\big) = \begin{cases} \mathcal{N}(\mu,\,\sigma^2) & \text{if } \ \sigma > 0 \\ \mathcal{N}(\mu,\,\sigma^2) \circledast f(R_i) & \text{if } \ \sigma \leq 0 \end{cases} \tag{4}$$

where

$$f(R_i) = \begin{cases} 1 & \text{if } \ R_i < 3\sigma_{ul} \\ 0 & \text{if } \ R_i > 3\sigma_{ul} \end{cases} \tag{5}$$

The second term of the integral in Equation 3 describes the probability of obtaining the intrinsic abundance ratio given the IMF defined in Equation 1 combined with the nucleosynthesis calculations of the ejecta of the enriching stars. We utilise the yields from HW10 to construct the expected distribution of chemical abundances given an underlying IMF model.

In our analysis, we consider the [C/O], [Si/O], [Al/O], and [Fe/O] abundance ratios. Therefore, for a given enrichment model, the probability of a system's chemical composition is given by the joint probability of these four abundance ratios.

Our model contains six parameters: $N_\star$, α, $M_{\rm min}$, $M_{\rm max}$, $E_{\rm exp}$ and $f_{\rm He}$. In the case of a well-sampled IMF, $R_i = R_m$; however, as the first stars are thought to form in small multiples (Turk et al. 2009; Stacy et al. 2010), the number of enriching stars is expected to be small. Thus, the IMF of the first stars is stochastically sampled. Due to the stochasticity of the IMF, we have to construct abundance ratio probability distributions, $p(R_i|R_m)$, for each combination of our fiducial model parameters. The range of model parameters we consider are:

$$\begin{aligned} 1 \leq \quad & N_\star \quad \leq 100 \ , \\ 0.3 \leq & E_{\rm exp}/10^{51}{\rm erg} \leq 10 \\ 0 \leq \ & f_{\rm He} \leq 0.25 \ . \end{aligned}$$

[5] i.e. the first local measurement of the stellar IMF (Salpeter 1955). See Chabrier (2003) for an alternative functional form.

In what follows, we assume that stars with masses > 10 M$_\odot$ are physically capable of undergoing core-collapse. Therefore, this parameter is fixed at a value $M_{\rm min} = 10$ M$_\odot$. We also consider a maximum mass, $M_{\rm max}$, above which all stars are assumed to collapse directly to a black hole, and do not contribute to the chemical enrichment of their surroundings. We impose a uniform prior of $20 < M_{\rm max}/{\rm M}_\odot < 70$ on the maximum mass of the enriching stars — this upper bound corresponds to the mass limit above which pulsational pair-instability SNe are believed to occur (Woosley 2017). α is assumed to be Salpeter. Similarly, we impose a uniform prior on the explosion energy, a choice that is driven by the yield set utilised in this analysis. We describe these nucleosynthesis yields in more detail in the following section. The explored range of $E_{\rm exp}$ covers all feasible explosion energies given our current understanding of core-collapse SNe.

4. DISCUSSION

4.1. *Comparison with UFDs*

We now compare the chemistry of this DLA to the chemistry of stars that have been detected in surrounding ultra faint dwarf galaxies (UFDs; $M_{\rm V} > -7.7$ from Simon (2019) definition). We adopt the solar scale Fe$_\odot = 7.47$. In stellar studies it is typical to assume Fe$_\odot = 7.51$. On this scale our Fe limit would be [Fe/H] < -3.70. The lowest mean metallicity of a confirmed UFD is that of Tucana II with [Fe/H] $= -2.9^{+0.15}_{-0.16}$ (Bechtol et al. 2015; Walker et al. 2016; Chiti et al. 2018; Simon 2019). The gas

There are 5 stars within UFDs with [Fe/H] abundances lower than our reported upper limit. These are found in Segue 1, Usra Major I, and Canes Venatici II, with [Fe/H] $= -3.78 \pm 0.11$, -3.91 ± 1.15, -4.2 ± 1.08, -3.88 ± 0.3, and -3.94 ± 0.96. There is only one with an associated error less than 5 per cent. This is SDSS J10063933+1600086 commonly known as Seg 1 161 (Simon et al. 2011). The star in question has a reported [CH/Fe] $= +0.91 \pm 0.25$ and [Si/Fe] $= +1.27 \pm 0.25$ (note: need to email AF to get exact error for this star - errors based that in SAGA database - did they take example from Table 5 or ask for exact errors? Frebel et al. 2014). To perfectly compare the metallicity of this star to our DLA required the detection of the same elements across each system. This is not currently possible. We therefore adopt a metallicity indicator that is the median [X/H] abundance determined from all of the detected elements out of C, O, Si, and Fe (i.e. all of those accessible for metal-poor DLAs 0

A EMP star that is not C-enchanced star has been detected in Boötes I with [Fe/H] $= -3.66 \pm 0.11$ (Fe solar = 7.51; Norris et al. 2010). This object has a comparable [C/H] abundance to that of our DLA [C/H] $= -3.45 + -0.20$ (determined from CH) compared to our [C/H]$= -3.42 \pm 0.07$. The abundances of the other mutual elements are: [O/H] < -1.75, [Si/H] $= -2.89$, and [Al/H] $= -4.35 \pm 0.11$. Figure 4 visualises this comparison.

TO DO:

- Use the inferred enrichment model to construct expected yield of all elements and hence determine the *total* metallicity of the system. Repeat for Boo-1137 and Segue 1 stars (C-enhanced). Compare :)
- Selection effect for less C-enhanced stars in UFDs???
- Calculate gas mass and stellar mass.
- Focus on the evolution of what this object will be — relative fractions of these can be predicted from simulations. UFDs redshift, quenching, density, temperature, warm neutral gas. What does it imply? Can't get density from Si III

5. CONCLUSIONS

We present the updated chemical abundances of the the DLA towards J0903+2628 based on data collected with Keck I/HIRES. These data reaffirm that this gas reservoirs is the most metal-poor DLA currently known/ Our main conclusions are are follows:

1. The latest data suggest [Fe/H]≤ -3.66 (2σ). This is a 0.85 dex improvement on the previous upper limit and confirms that this DLA is indeed EMP. To secure the first firm detection of iron in this system will require further observations. This would require a significant time investment on $8 - 10$ m class telescopes. However, will be efficiently achieved with the next generation of $30 - 40$ m telescopes.
2. We present the first limit on the abundance of an odd-atomic number element for this DLA; [Al/H] < -3.66 (2σ). Note the abundances of the other accessible elements are consistent with the previous determination. Al is a useful discriminant of the explosion mechanism of the enriching stellar population.
3. We compare the chemistry of this DLA to the abundances of the most metal-poor stars in the

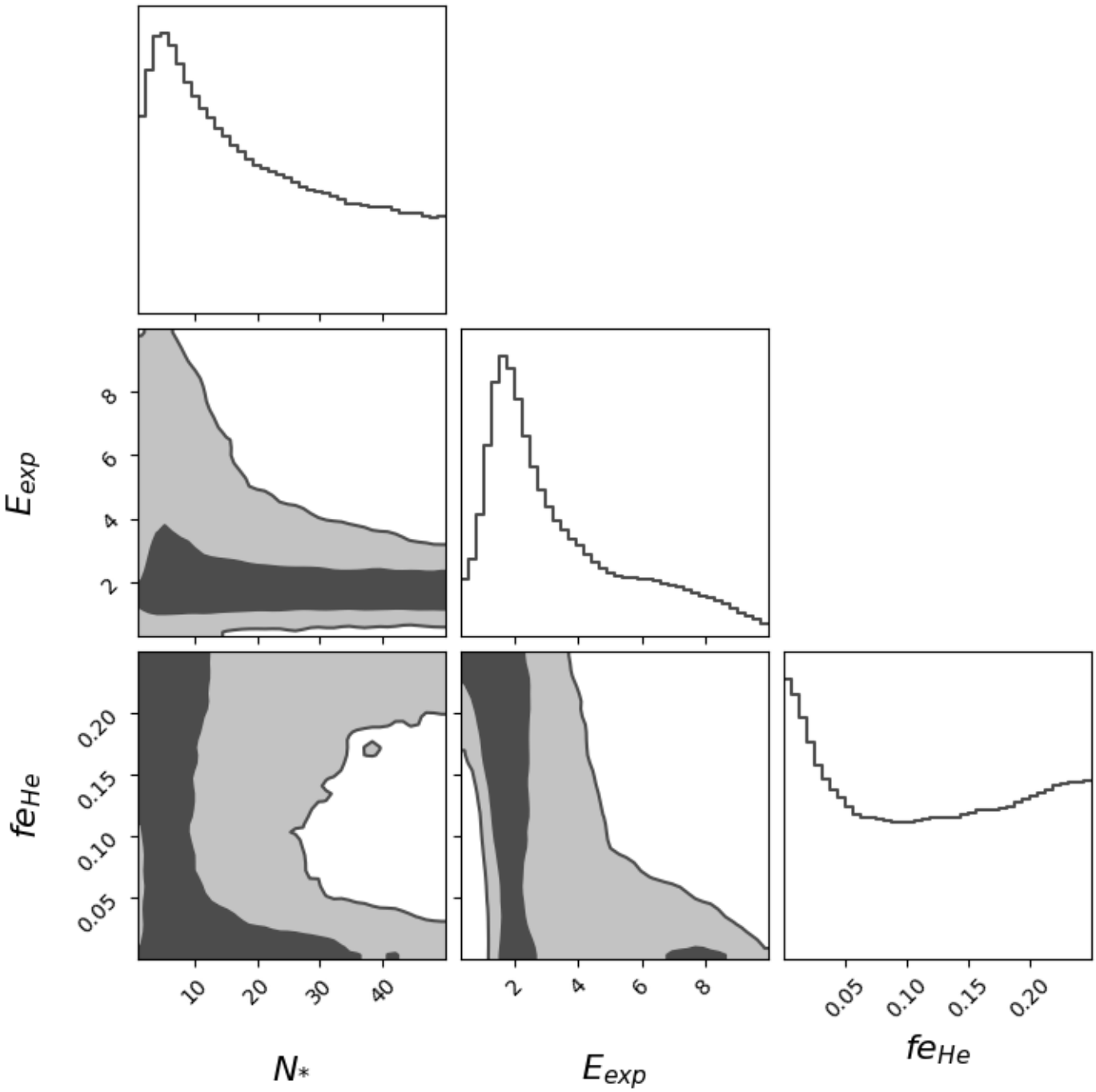

Figure 2. Placeholder till model is run properly! Not converged

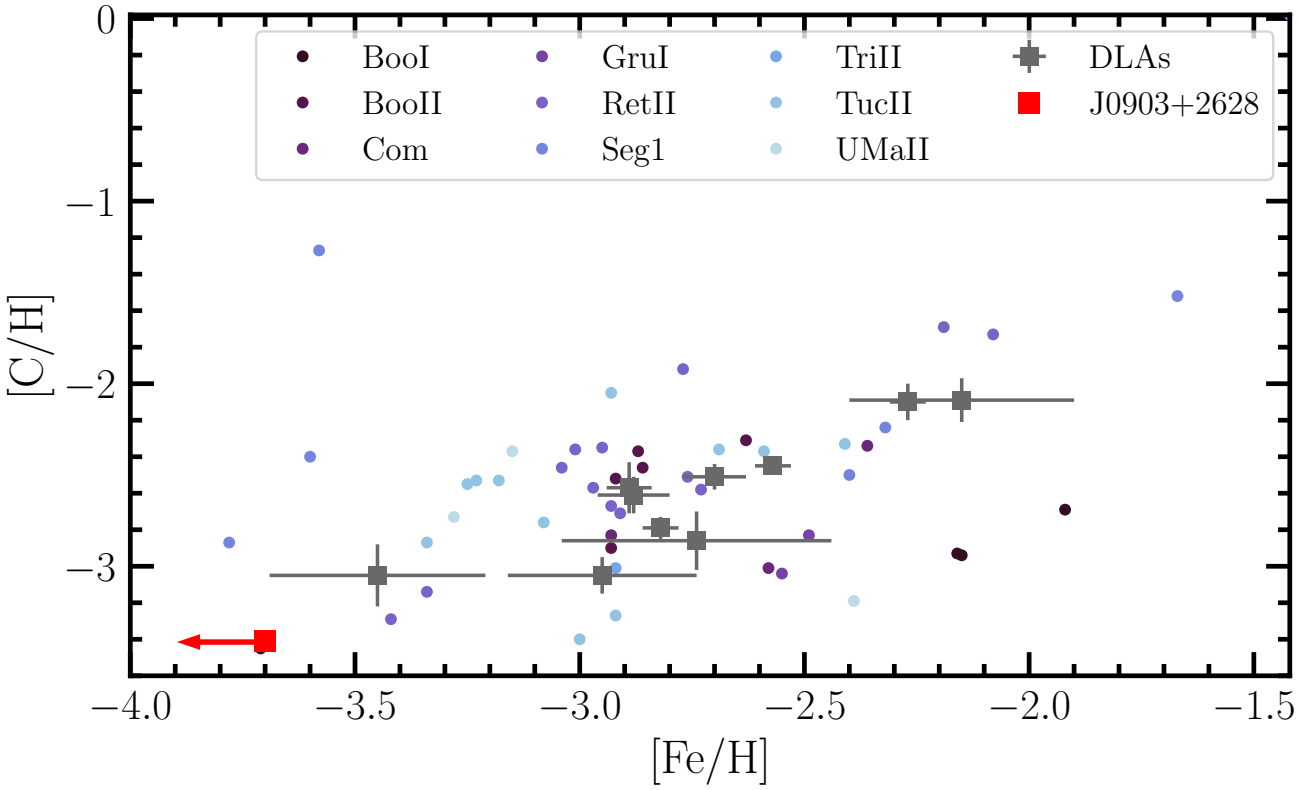

Figure 3. These are the [C/H] vs [Fe/H] abundances of stars in ultra faint dwarf galaxies. It is not necessarily complete - from SAGA database and includes: Bootes I, Bootes II, Canes Venatici II, Coma Berenices, Grus I, Grus II, Leo IV, Leo V, Pisces II, Tucana II, Tucana III, Ursa Major, and Willman I. Given table from Simon 2019 sup material, we are missing: Crater II, Virgo I, Hydra II, Draco II, Sagittarious II, Indus II, Pegasus III, Aquarius II, Tucana V, and Phoenix II.

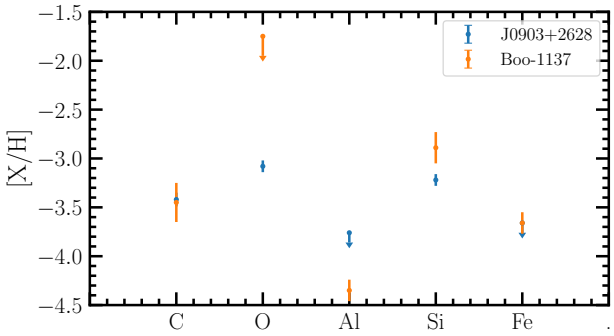

Figure 4. Comparisons of the [X/H] abundances of the common chemical elements detected for J0903+2628 and Boo−1137.

UFDs orbiting the Milky Way. The limit on the [Fe/H] abundance of this system is lower than that of any star in these UFDs. The closest comparison is Boo−1137 in Boötes I with [Fe/H] = −3.62±0.11 (registered onto our adopted solar scale Norris et al. 2010). Comparing the [X/H] abundances of common elements across these relics shows a broadly consistent chemistry. This may suggest that the DLA is the gas from which some stars in the UFDs form.

4. Chemical enrichment model suggests low N and the properties of the individual star is?

5. This is a great target for JWST :D

This paper is based on observations collected at the W. M. Keck Observatory which is operated as a scientific partnership among the California Institute of Technology, the University of California and the National Aeronautics and Space Administration. The Observatory was made possible by the generous financial support of the W. M. Keck Foundation. The authors wish to recognize and acknowledge the very significant cultural role and reverence that the summit of Maunakea has always had within the indigenous Hawaiian community. We are most fortunate to have the opportunity to conduct observations from this mountain. We are also grateful to the staff astronomers at Keck Observatory for their assistance with the observations. This work has been supported by Fondazione Cariplo, grant No 2018-2329. During this work, R. J. C. was supported by a Royal Society University Research Fellowship. We acknowledge support from STFC (ST/L00075X/1, ST/P000541/1). This project has received funding from the European Research Council (ERC) under the European Union's Horizon 2020 research and innovation programme (grant agreement No 757535). This work used the DiRAC Data Centric system at Durham University, operated by the Institute for Computational Cosmology on behalf of the STFC DiRAC HPC Facility (www.dirac.ac.uk). This equipment was funded by BIS National E-infrastructure capital grant ST/K00042X/1, STFC capital grant ST/H008519/1, and STFC DiRAC Operations grant ST/K003267/1 and Durham University. DiRAC is part of the National E-Infrastructure. This research has made use of NASA's Astrophysics Data System.

Facilities: Keck:I (HIRES)

Software: Astropy (Astropy Collaboration et al. 2013), Corner (Foreman-Mackey 2016), Matplotlib (Hunter 2007), and NumPy (van der Walt et al. 2011).

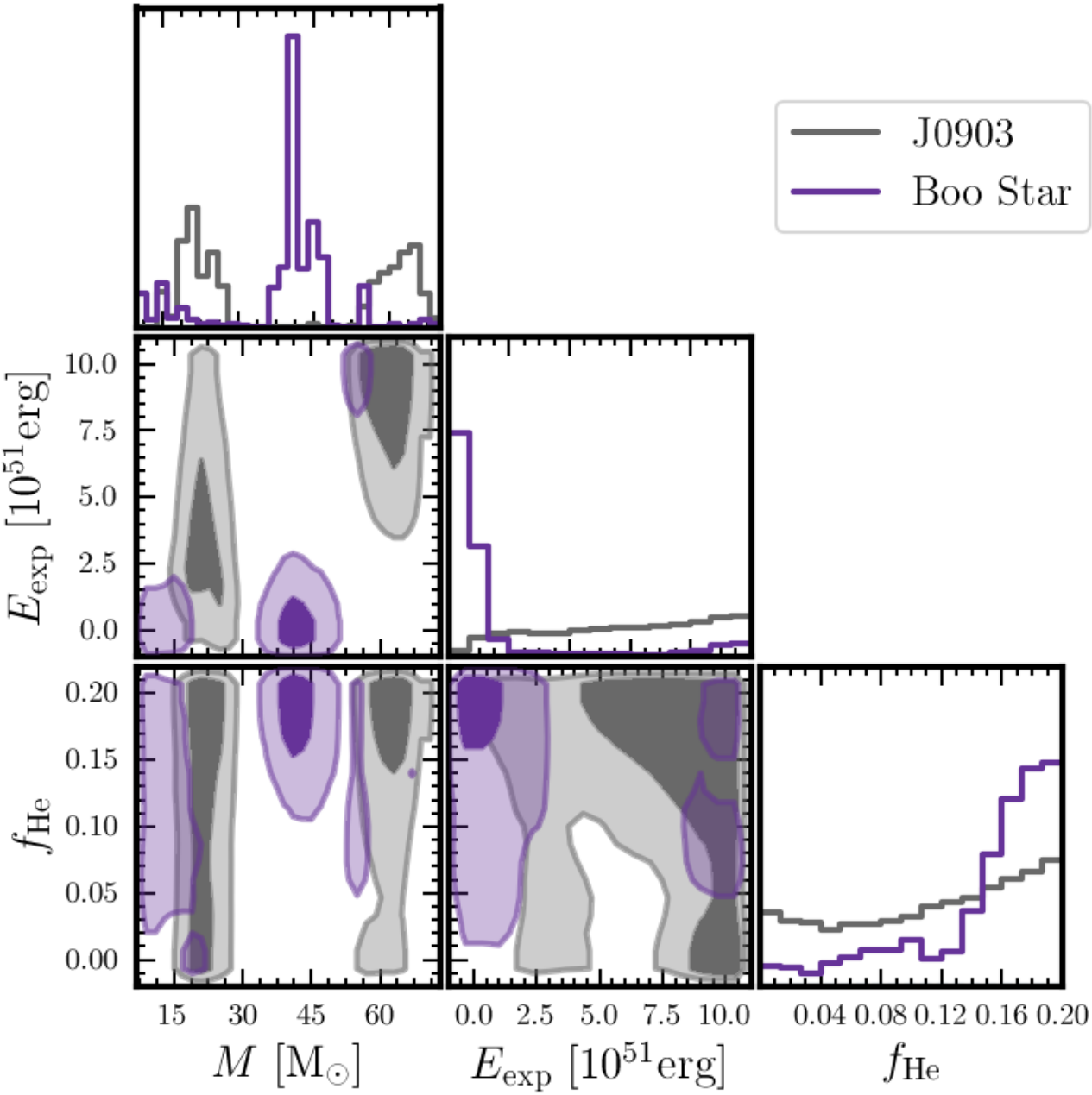

Figure 5. Comparisons inferred Population III properties for J0903+2628 and Boo−1137. Is it interesting enough to include?? What we learn: - broadly similar but star more well constrained. Bias from simulations being based on observed stellar abundances? Or, star better modelled by individual enrichment event than DLA?

REFERENCES

Astropy Collaboration, Robitaille, T. P., Tollerud, E. J., et al. 2013, A&A, 558, A33, doi: 10.1051/0004-6361/201322068

Bechtol, K., Drlica-Wagner, A., Balbinot, E., et al. 2015, ApJ, 807, 50, doi: 10.1088/0004-637X/807/1/50

Beers, T. C., & Christlieb, N. 2005, ARA&A, 43, 531, doi: 10.1146/annurev.astro.42.053102.134057

Bosman, S. E. I., & Becker, G. D. 2015, MNRAS, 452, 1105, doi: 10.1093/mnras/stv1336

Chabrier, G. 2003, PASP, 115, 763, doi: 10.1086/376392

Chiti, A., Frebel, A., Ji, A. P., et al. 2018, ApJ, 857, 74, doi: 10.3847/1538-4357/aab4fc

Cooke, R. J., Pettini, M., & Jorgenson, R. A. 2015, ApJ, 800, 12, doi: 10.1088/0004-637X/800/1/12

Cooke, R. J., Pettini, M., & Steidel, C. C. 2017, MNRAS, 467, 802, doi: 10.1093/mnras/stx037

Foreman-Mackey, D. 2016, The Journal of Open Source Software, 1, 24, doi: 10.21105/joss.00024

Frebel, A., Simon, J. D., & Kirby, E. N. 2014, ApJ, 786, 74, doi: 10.1088/0004-637X/786/1/74

Heger, A., & Woosley, S. E. 2010, ApJ, 724, 341, doi: 10.1088/0004-637X/724/1/341

Hunter, J. D. 2007, Computing in Science and Engineering, 9, 90, doi: 10.1109/MCSE.2007.55

Norris, J. E., Yong, D., Gilmore, G., & Wyse, R. F. G. 2010, ApJ, 711, 350, doi: 10.1088/0004-637X/711/1/350

Noterdaeme, P., Balashev, S., Ledoux, C., et al. 2021, arXiv e-prints, arXiv:2105.00697. https://arxiv.org/abs/2105.00697

Péroux, C., & Howk, J. C. 2020, ARA&A, 58, 363, doi: 10.1146/annurev-astro-021820-120014

Salpeter, E. E. 1955, ApJ, 121, 161, doi: 10.1086/145971

Simcoe, R. A., Sullivan, P. W., Cooksey, K. L., et al. 2012, Nature, 492, 79, doi: 10.1038/nature11612

Simon, J. D. 2019, ARA&A, 57, 375, doi: 10.1146/annurev-astro-091918-104453

Simon, J. D., Geha, M., Minor, Q. E., et al. 2011, ApJ, 733, 46, doi: 10.1088/0004-637X/733/1/46

Stacy, A., Greif, T. H., & Bromm, V. 2010, MNRAS, 403, 45, doi: 10.1111/j.1365-2966.2009.16113.x

Turk, M. J., Abel, T., & O'Shea, B. 2009, Science, 325, 601, doi: 10.1126/science.1173540

van der Walt, S., Colbert, S. C., & Varoquaux, G. 2011, Computing in Science and Engineering, 13, 22, doi: 10.1109/MCSE.2011.37

Walker, M. G., Mateo, M., Olszewski, E. W., et al. 2016, ApJ, 819, 53, doi: 10.3847/0004-637X/819/1/53

Welsh, L., Cooke, R., & Fumagalli, M. 2019, MNRAS, 487, 3363, doi: 10.1093/mnras/stz1526

Welsh, L., Cooke, R., Fumagalli, M., & Pettini, M. 2020, MNRAS, 494, 1411, doi: 10.1093/mnras/staa807

Wolfe, A. M., Gawiser, E., & Prochaska, J. X. 2005, ARA&A, 43, 861, doi: 10.1146/annurev.astro.42.053102.133950

Woosley, S. E. 2017, ApJ, 836, 244, doi: 10.3847/1538-4357/836/2/244